Technical Paper

Transactions of the Society of
Naval Architects of Korea
Vol.28, No.2, October 1991
大 韓 造 船 學 會 論 文 集
第28券 第2號 1991年 10月

Vortex-Induced Vibration of Flexible Cylinders Having Different Mass Ratios

by
Chung, Tae-Young*

원통형 부재의 질량비에 따른 와유기진동 특성연구

정태영*

Abstract

A series of experiments were performed to see the dependence of the response characteristics of vortex-induced vibration of flexible cylinders on mass rations for marine applications. Experiments were conducted in the 60cm × 60cm test section of the cavitation tunnel at the Korea Research Institute of Ships and Ocean Engineering using 5 test rods of 60cm length and 6mm diameter with different mass ratios. It was confirmed quantitatively from the experiments that the low mass ratio cylinders have much broader flow velocity range of large amplitude vibrations than high mass ratio ones.

요 약

유체흐름중에 있는 원통형부재의 질량비에 따른 와유기진동특성을 파악하기 위하여 일련의 시험이 수행되었다. 실험은 질량비가 서로 다른 5개의 시험봉(길이 60cm:직경 6mm)을 제작하여 해사기술연구소의 공동수조에서 실시하였다. 주요 실험결과로서 원통형부재에 고진동을 유발하는 유체속도의 범위는 질량비에 따라 변화하며, 가벼운 원통형부재가 무거운 원통형부재에 비하여 더 넓은 유체속도 범위에 걸쳐 고진동현상을 나타냄이 정량적으로 밝혀졌다.

발표 : 1990년도 대한조선학회 추계연구발표회 ('90. 11.10)
Manuscript received : January 10, 1991, revised manuscript received : March 22, 1991.
* Member, Korea Research Institute of Ship and Ocean Engineering

1. Introduction

If the cylinder is flexible or flexibly mounted, interaction may arise between the vortex-shedding mechanism and the cylinder oscillation. The well known phenomenon caused by this interaction is lockin(or synchronization) of the vortex shedding frequency to the structure's vibrating frequency(usually a structural natural frequency). At lockin, structural oscilation is synchronized to the vortex shedding frequency often resulting in increased strucrtural response. The increase in cylinder oscillation is restricted by self-limiting decreases in vortex strength and increases in fluid damping due to large oscillation of the cylinder.

Although many successful experiments have been made to understand the lockin phenomena and many authors have given comprehensive reviews related to the lockin phenomena [1, 2, 3, 4], some of the lockin phenomena are still quite unclear. One of them is that the relation between lockin range and other non-dimensional parameters. Generally, it is known that the low mass ratio cylinders have much broader lockin ranges than high mass ratio ones[5, 6], but this has not been confirmed quantitatively yet. The mass ratio is a measure of the mass per unit length of the cylinder compared to the mass per unit length of displaced fluid as generally defined by:

$$\mu = \frac{m}{\rho_w D^2} \tag{1}$$

where,

μ = mass ratio

m = mass per unit length of flexible cylinder

ρ_w = water density

D = cylinder out-diameter

In this study, a series of experiments were performed to see the relation between the response characteristics of vortex-induced vibration of flexble cylinders and mass ratios for marine application.

2. Experiments

2.1 Experimental Setup

Experiments were conducted in the 60cm × 60 cm test section of the cavitation tunnel at the Korea Research Institute of Ships and Ocean Engineering(KRISO). The maximum capacity of flow speed of the water tunnel is up to 12 m/sec.

Five different test rods having different mass ratios were prepared. All the test rods have 60 cm length and 6mm diameter. The important properties of the test rods are summarized in Table 1.

The test rods were mounted in the test section of the cavitation tunnel as shown in Fig.1 with the fixed boundary conditions at both ends. Two pairs of strain gages at the top and bottom sides of the test rod were bonded in a half bridge configuration at 30mm apart from both ends.

Table 1 Specification of test rods

Test rod No.	Length (cm)	out-diameter (mm)	Wall thickness (mm)	Mass ratio	Remarks
1	60	6.0	0.4	1.6	-
2	〃	〃	0.4	2.6	Coaxial Cable (RG-58) inside of the rod
3	〃	〃	0.9	3.3	-
4	〃	〃	0.4	5.0	Small lead balls inside the rod
5	〃	〃	full	6.1	-

2.2 Test Procedure

After the test rod was completely mounted, the impact test was carried out to get natural frequencies and damping information of the test rod in air. Then, water was filled in the tunnel and the water was circulated at the lowest possible velocity by controlling the impeller rpm of the tunnel. When the flow was stabilized, the first test was begun. Current output proportional to pressure difference between upstream and downstream of contraction part of the tunnel was read to estimate the flow velocity. The flow velocity was estimated from the calibration chart relating the current outputs to the flow velocities. The Propulsor Technology Lab. of KRISO provided the calibration chart of it. The tape recorder(TEAC R-260LT) was turned on and voltage outputs from strain amplifiers (HBM;AE3407B)were recorded. After a sufficient amount of data has been taken, the flow velocity was increased and the cycle was repeated until the planned maximum flow velocity was obtained.

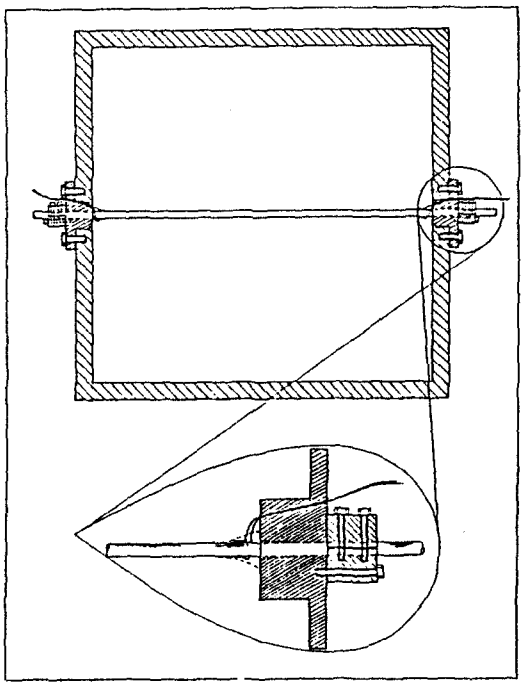

Fig. 1 Test set-up

2.3 Measuring and Processing System

A schematic diagram of the instrumentation system is shown in Fig.2. Dynamic strain signals recorded on tape were processed using spectrum analizer(HP 3582A) and IBM/PC-compatible. Flat top window giving more correct amplitude of signals than other windows was used to get strain spectra from the spectrum analyzer. Sampling frequency for data processing was 1,024Hz and the number of data in a process was 1,024 so that the time record length for a process was 1 second. The number of averaging of the spectra was 4. These obtained strain spectra were stored in IBM/PC-AT compatible through GP-IB interface and were plotted using a laser printer(QNIX QLBP -2000)

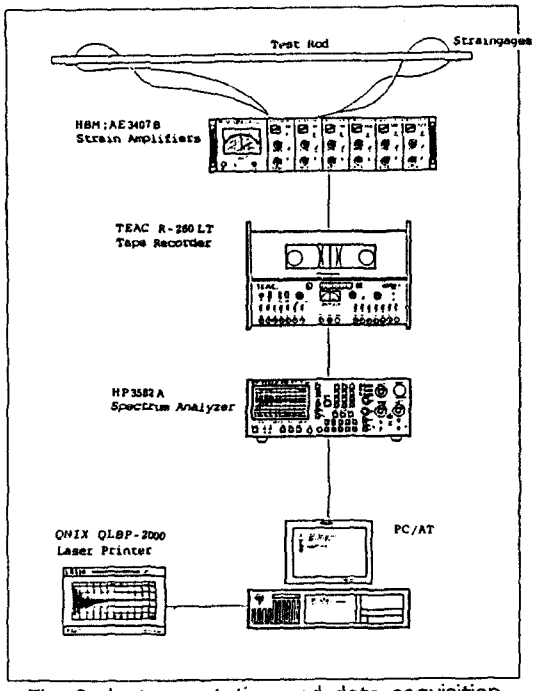

Fig. 2 Instrumentation and data acquisition schematic

3. Experimental Results

3.1 Natural Frequencies and Damping Ratios of the Test Rods

The natural frequencies and damping ratios of the test rods in air measured from impact tests are summarized in Table 2. Table 2 also includes the calculated natural frequencies of the test rods in air assuming the fixed boundary conditions at both ends. The measured natural frequencies are about 0.9 times of the calculated ones. This may come from the imperfect fixed boundary conditions of the mount of the test rods.

If we model the mounted test rod as a pinned -pinned beam with rotational spings at both ends, the natural frequencies of the test rod are calculated as follows:

$$f_n = \frac{\lambda_n^2}{2\pi\ell^2}\left(\frac{EI}{m}\right)^{\frac{1}{2}} \qquad (2)$$

where,

f_n = natural frequency of the nth mode

m = mass per unit length

EI = bending rigidity

l = beam length

λ_n = parameter depending on the rotat -ional spring constant

Table 2 Natural frequencies and damping ratios of test rods

Test rod No.	Natural Frequencies (Hz)			Damping ratio (ζ_1)
	f_1	f_2	f_3	
1	92.2 (101)*	253 (278)	491 (545)	0.005
2	70.6 (77.4)	193 (213)	376 (418)	0.007
3	81.8 (91.0)	228 (251)	446 (491)	0.005
4	49.6 (56.3)	136 (155)	268 (304)	0.006
5	68.0 (77.1)	184 (212)	352 (417)	0.005

* Values in ( ) represent the calcuulated natural frequencies with fixed bounday conditions at both ends.

A pinned-pinned beam with infinite rotational spring constants at both ends corresponds to a fixed-fixed beam. The value of λ_1 for the fundamental mode of a fixed-fixed beam is known to be 4.73 and the fundamental natural frequency is given by:

$$f_{1\infty} = \frac{4.73^2}{2\pi\ell^2}\left(\frac{EI}{m}\right)^{\frac{1}{2}} \qquad (3)$$

From Eq.(2) and Eq.(3), the ratio $\frac{f_1}{f_{1\infty}}$ is given by:

$$\frac{f_1}{f_{1\infty}} = \frac{\lambda_1^2}{4.73^2} \qquad (4)$$

In the case of $\frac{f_1}{f_{1\infty}} = 0.9$ Eq.(4) gives the value of λ_1 as 4.49. The rotational spring constant κ can be obtained in a reverse way from the table in [7] and it is found that the value of $\frac{\kappa l}{EI}$ is roughly a little lower than 100.

The rotational spring constanst at the both ends of the test rods can be estimated in another way. The relationship between the displacement at the center and the strain at the measured point can be obtained analytically as follow:

$$\delta = \frac{l^2}{12D}\left[\frac{\frac{4(2+a)}{a}-3}{1-\frac{2+a}{5a}}\right]\varepsilon \qquad (5)$$

where,

δ = displacement at the center(㎜)

ε = strain at the measured point

$a = \frac{\kappa l}{EI}$

For the estimation of a, the displacement at the center was also measured with strain measurements when the static loading was given at the center. The measured displacement at the center in ㎜ was linearly proportional to the measured strain with the proportional constant of 6,800 and the estimated value of a was 97.

3.2 Strain Spectra

Strain spectral maps were obtained from experiments and Fig.3 shows the result for the test rod 5 which has the largest mass ratio of 6.

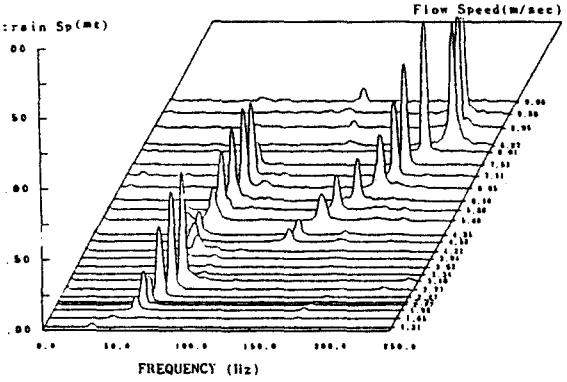

Fig. 3 Stain Spectral map obtained from straingaqes bomded on Test Rod 5 ($m/\rho_w D^1=6.1$)

1. X-axis, Y-axis and Z-axis in this figure represent frequency, RMS strain amplitude and the flow speed at which each strain spectrum was obtained, respectively.

Strain amplitudes and vibrating frequencies of the main components of the strain spectra are plotted versus reduced velocity in from Fig. 4(a) to Fig.4(e). Reduced velocity is defined by $V_r = U/f_1 D$ where U is flow velocity, D is the cylinder diameter, and f_1 is the measured fundamental natural frequency of the test rods in air.

3.3 Estimation of the Displacement at the Center of the Test Rods

The maximum vibration amplitude of the test rod at the center can be estimated from the measured strains.

The fundamental mode of a pinned beam with rotational springs at both ends is given by [8]:

$$\Psi_1(\chi) = c_1\left(cosh\frac{\lambda_1\chi}{l} - cos\frac{\lambda_1 x}{l}\right) + c_2 sin\, h\frac{\lambda_1 x}{l} + sin\,\frac{\lambda_1 x}{l} \qquad (6)$$

where,

$$C_1 = -cot\frac{\lambda_1}{2}$$

$$C_2 = cot\frac{\lambda_1}{2} tan\, h\frac{\lambda_1}{2}$$

The relation between the measured strains at $x = l/20$ and $x = 19l/20$ and the maximum vibration amplitude at the center for the first mode vibration is given by:

$$\frac{A}{\varepsilon} = \frac{2}{D}\frac{\Psi_1(l/2)}{\Psi''_1(l/20)} \qquad (7)$$

where,

A = maximum vibration amplitude at the center

ε = meaured strains at $x = l/20$ or $x = 19l/20$

$\Psi_1(l/2)$ = the value of the first mode shape at $x=l/2$

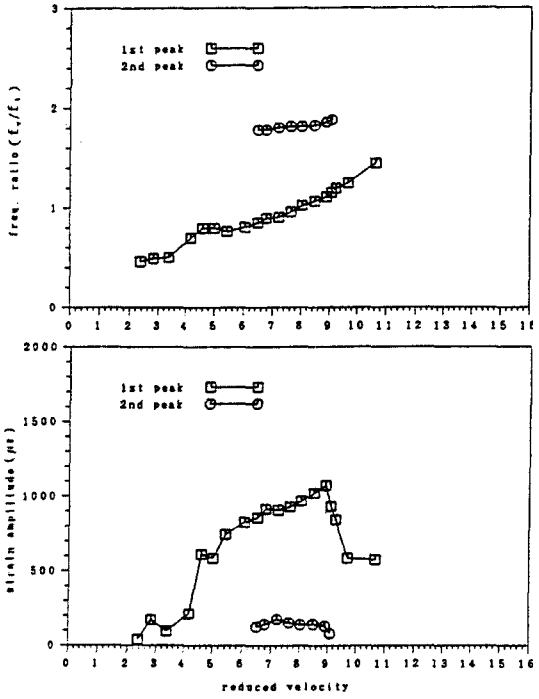

Fig. 4 (a) Peak frequency and strain amplitude of vortex-induced vibration versus reduced velocity (Test Rod 1; $m/\rho_w D^2 = 1.6$)

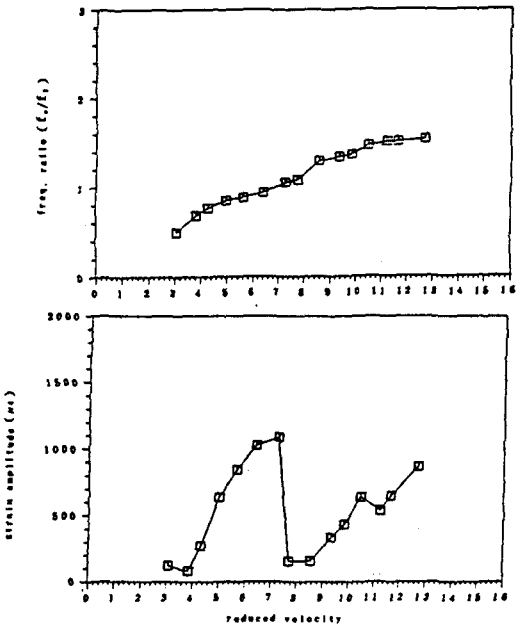

Fig. 4 (b)Peak frequency and strain amplitude of vortex-induced vibration versus reduced velocity (Test Rod 2;$m/\rho_w D^2$ =2.6)

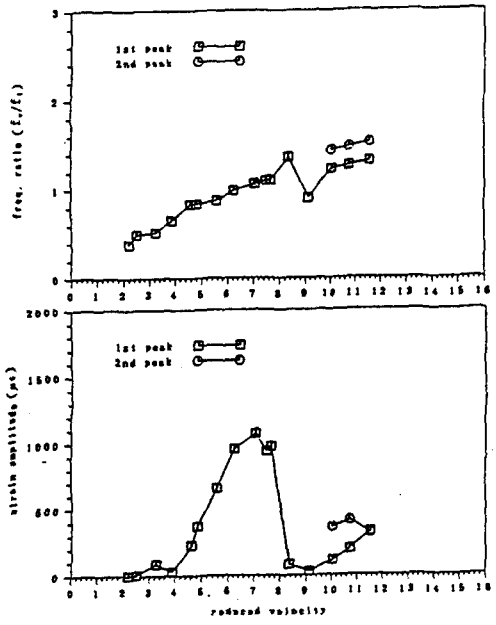

Fig. 4 (c) Peak frequency and strain amplitude of vortex-induced vibration versus reduced velocity(Test Rod 3;$m/\rho_w D^2$ =3.3)

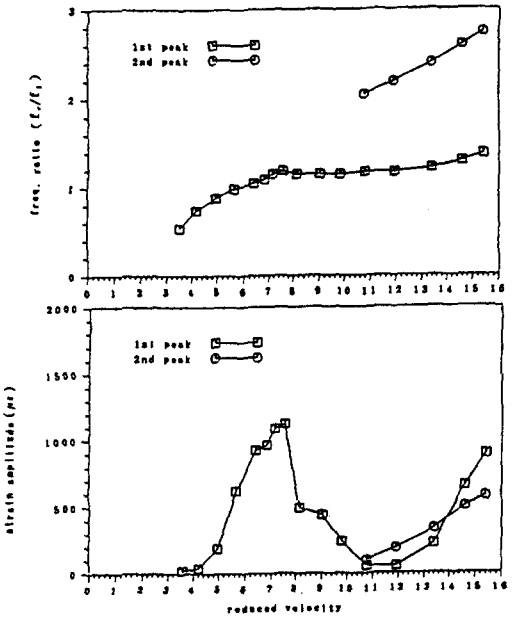

Fig. 4 (d) Peak frequency and strain amplitude of vortex-induced vibration versus reduced velocity(Test Rod 4;$m/\rho_w D^2$= 5.0)

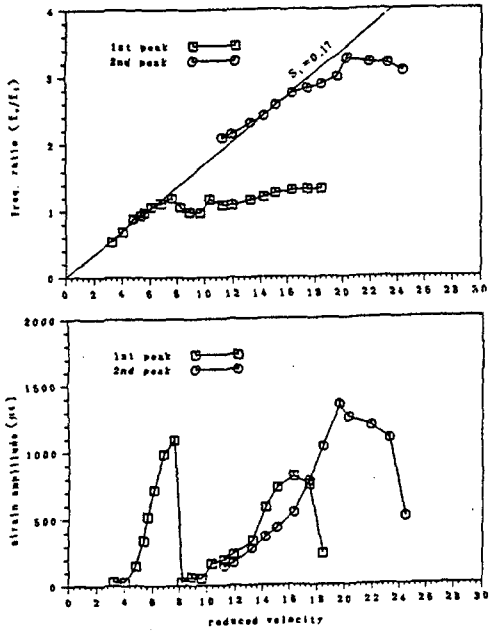

Fig. 4 (e) Peak frequency and stain amplitude of vortex-induced vibration versus reduced velocity(Test Rod 5;$m/\rho_w D^2$ =6.1)

$\Psi_1''(l/20)$ = the value of spatial second derivative of the first mode at $x=l/20$

Therefore, the vibration ampitude of the first mode at the center is obtained from Eq(6) and Eq(7) by putting $\lambda_1 = 4.49$ into those equations:

$$A[mm] = 7{,}200\,\varepsilon \qquad (8)$$

The vibration amplitude at the center estimated from the above equation is plotted versus reduced velocity for the test rods with different mass ratios in Fig.5.

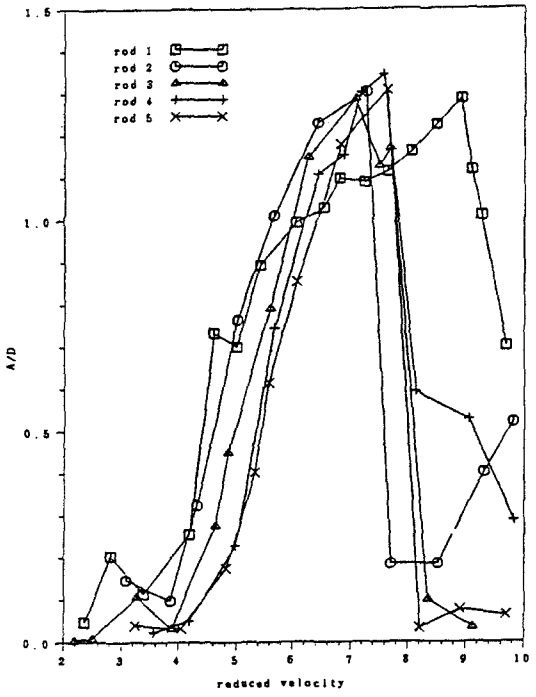

Fig. 5 Estimated displacements at the center of the test rods versus reduced velocity

4. Discussions

4.1 Vibration Frequency Characteristics

(1) It is known that the vibration frequency of the cylinder in the lockin region is almost constant and has the value of the natural frequency of the structure. However, the experimental results in Figs 4(a)-4(e) show that the vibration frequency does not remain constant but varies even in the lockin region. For example, in the case of Test Rod 1 in Fig.4(a), frequency ratios continue to increase from about 0.8 to about 1.2 as the reduced velocity increases from 4.5 to 9.0. Same trends were found in the case of the other test rods. This variation of the vibration frequency in the lockin region can be explained by introducing varying added mass coefficients on the basis of the assumption that the vibration frequency at lockin is a real natural frequency of the test rod in that instance. The variation in the fundamental natural frequency in water with varying added masses is given by:

$$f_{1,water} = f_1 \times \sqrt{\frac{1}{1+\frac{\pi C_m}{4\mu}}} \qquad (9)$$

where,

$f_{1,water}$ = fundamental natural frequency in water

f_1 = fundamental natural frequency in air

μ = mass ratio

C_m = added mass coefficient

Sarpkaya's experimental results [9, 10] show that the added mass coefficients of the compulsorily vibrating cylinder in steady flow are much larger than 1 for reduced velocities less than 5, and dramatically dropping to -0.5 for reduced velocity about 5.5 as shown in Fig.6. It is noted that the reduced velocity defined in this figure is $V_r = UT/D$, where T represents the period of the cylinder oscillation.

Inversely estimated added mass coefficients from the first peak frequency data in figs. 4(a)-4(e) using Eq.(9) is plotted as a function of reduced velocity in Fig. 7. This figure has much similarity to the Sarpkaya's result in Fig.6.

(2) At the end of the lockin range, the test rods oscillate at two different vibrating frequen-

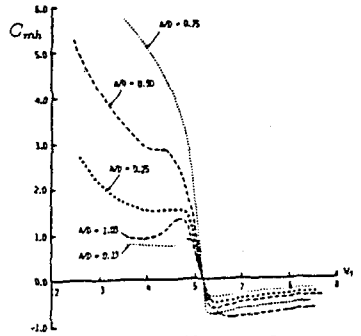

Fig. 6 Inertia coefficient C_{mh} versus reduced velocity for various amplitudes(from Ref.[9]and[10])

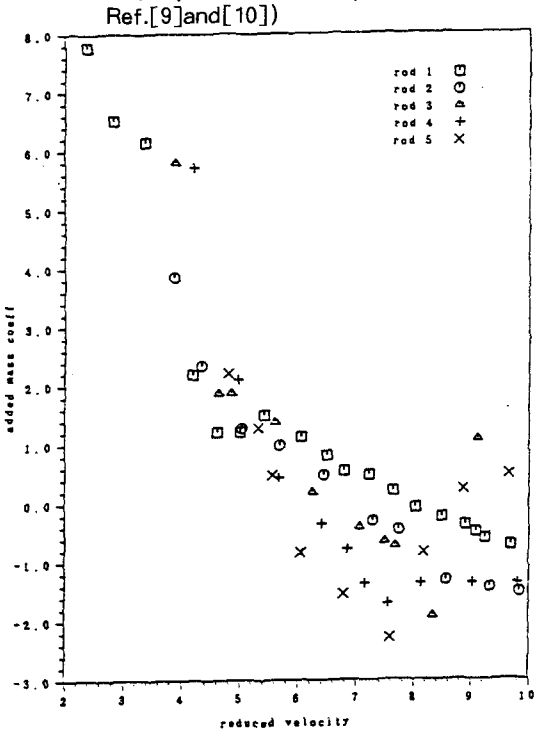

Fig. 7 Estimated added mass coefficients versus reduced velocity

cies as clearly shown in Fig.4(e). One frequency corresponds to the frequency governed by Strouhal relationship and another frequency corresponds to the natural frequency of the test rods. This also shows that vortex-induced vibration is not the simple forced vibration problem excited only by Strouhal frequency.

(3) Strictly speaking, the Strouhal number is defined only for stationary cylinders and the value of Strouhal number is almost constant, about 0.2 for a broad range of Reynolds number. However, as we can see from the result of Fig.4(e), the equivalent Strouhal number in flexible vibrating cylinders is about 0.17.

4.2 Vibration Amplitude Characteristics

Important observations that one can draw from Fig.5 are as follows:

(1) It was confirmed that low mass ratio rods have much broader lockin range than high mass ratio ones. Especially, the lockin range of Test Rod 1 having the least mass ratio of 1.6 extends over $4.5 < V_r < 9.5$. The lockin range of Test Rod5 having the largest mass ratio of 6.1 extends over $5.5 < V_r < 8.0$

This can be also explained by introducing the varying addecd mass coefficients. The added mass coefficient decreases with increasing reduced velocity over the lockin range and this raises the natural frequency as given in Eq(9). This makes the natural frequency of the test rod is close to the vortex shedding frequency, which is proportionally increasing to the flow speed. This allows the lockin range to be broad. This effect is less for the test rod with high mass ratio than for low mass ratio ones, because the added mass is a small percentage of the total mass[6].

(2) Maximum response amplitude occurs almost at the end of lockin range and falls in the range of $6.5 < V_r < 8.0$ except the case of Test Rod 1 in which maximum response amplitude occurs at about $V_r = 9.0$.

(3) The levels of maximum response amplitudes are almost the same for all the test rods and they are about 1.3 times of the test rod diameter. This means that the maximum response amplitude does not much depend on mass ratio for marine applications.

5. Summary and conclusions

Impontant observations and conclusions obtained from the experiments are as follows :

(1) Lockin range is broad and strongly dependent upon mass ratio as shown below.

$m/\rho_w D^2$	Lockin range
1.6	$4.5 < V_r < 9.5$
6.1	$5.5 < V_r < 8.0$

Therefore, it could be concluded from this observation that the critical flow velocity for flexible cylinders in uniform flow is not limited to the vicinity of $U = 5 f_n D$ but in the broad range of $4.5 f_n D < U < 9.5 f_n D$ for marine applications and the low mass ratio cylinders have much broader range of the critical flow velocity than high mass ratio ones.

(2) Vibration frequency varies even in the lockin range. This observation together with the observation (1) can be explained by introducing a varying added mass coefficient.

(3) The equivalent Strouhal number in flexible cylinders is about 0.17. This number instead of 0.2 may be used to estimate a vortex shedding frequency of flexible cylinders.

(4) Maximum vibration amplitudes are about 1.3 times of the test rod diameter and they do not much dependent on mass ratios.

Acknowledgements

This work was sponsored by the Ministry of Science and Technology, Korea. I would like to thank Mr. Jong-Ahn Chung, Mr. Yong-Yun Nam and Mr. Boung-Mun Min for their helps during experiments. Thanks are also extended to the members of Propulsor Technology Lab. of KRISO.

References

[1] Sarpkaya, T. "Vortex Induced Oscillations. A selective Review", ASME Journal of Applied Mechanics, Vol.46, June 1979.

[2] Griffin, O.M. and Ramberg, S.E., "Some Recent Studies of Vortex Shedding with Application to Marine Tubulars and Risers", Journal of Energy Resources Technology, Vol. 104, March 1982.

[3] King, R., "A Review of Vortex Shedding Research and It's Application", Ocean Engineering, Vol.4, 1977.

[4] Blevins, R.D., *Flow-Induced Vibration*, Van Nostraned Reinhold Co., New York, 1977.

[5] Chung, T.Y., "Vortex-Induded Vibration of Flexible Cylinders in Sheared Flow", Ph. D. Thesis, Massachusetts Institute of Technology, Ocean Engineering Department, June 1987.

[6] Vandiver, J.K., "Predicting the Response Characteristics of Long, Flexible Cylinders in Ocean Currents", Ocean Structural Dynamics Symposium '88, Oregon State University, Sept., 1988.

[7] Blevins, R.D., *Formulas for Natural Frequency and Mode Shape*, Van Nostrand Reinhold Company, 1979.

[8] Carmichael, T.E., "The Vibration of a Rectangular Plate with Edges Elastically Restrained against Rotation", Quart. J. Mech. Appl. Math., 12, part 1,1959.

[9] Sarpkaya, T., "Transverse Oscillations of Circular Cylinder in Uniform Flow, Part 1", Report No. NPS-69SL77071-R, Naval Postgraduate School, Monterey, CA, December 25, 1977.

[10] Botelho, D.L.R., "An Empirical Model for Vortex-Induced Vibrations", Report No. EERL82-02, Calif. Institute of Technology, Earthquake Engineering Research Laboratory, August 1982.